CHAPTER IV

RESULTS AND DISCUSSIONS

This chapter is divided into three sections. The first section contains the details solubility of each vanadium salt used. The second section contains the characterization results obtained from the various characterization techniques i.e. X-ray fluorescence spectroscopy (XRF), X-ray diffraction (XRD), Fourier-transform infrared spectroscopy (FT-IR), Brunaur-Emmett-Teller (BET) surface area, pore volume and pore sized analysis, Scanning electron microscopy (SEM), Electron spin resonance (ESR) and NH_3-Temperature programmed desorption (NH_3-TPD). The last section contains the catalytic results of the gas phase oxidation of 2-propanol.

For convenience of discussion, the V/TS-1 catalysts with different in the vanadium salt addition method and vanadium source will be named as VCl_3_A1, VCl_3_A2, VCl_3_A1A2, VCl_3_B1, VCl_3_B2, VCl_3_C1, VCl_3_C2, $VO(acac)_2\_A1$, $VO(acac)_2\_A2$, $VO(acac)_2\_A1A2$, $VO(acac)_2\_B1$, $VO(acac)_2\_B2$, $VO(acac)_2\_C1$, $VO(acac)_2\_C2$, $V_2O_5\_A1$, $V_2O_5\_A2$, $V_2O_5\_A1A2$, $V_2O_5\_B1$, $V_2O_5\_B2$, $V_2O_5\_C1$, and $V_2O_5\_C2$ respectively. The chemical formula before the underscore line indicates the vanadium source used and the block letter followed by the number indicates the solution in which the vanadium compound was added.

4.1 The solubility

The solubility of each vanadium compound in A1, A2, B1, B2, C1 and C2 solution are shown in Table 4.1.

Table 4.1 The solubility of vanadium compounds

Vanadium compounds	Solubility					
	A1	A2	B1	B2	C1	C2
VCl_3	√	√	×	×	√	√
$VO(acac)_2$	√	√	×	×	×	×
V_2O_5	√	√	×	×	√	√

Where √ = soluble, × = insoluble

Table 4.1 indicates that all of vanadium compounds used in this study could not dissolved in either B1 or B2 solution, therefore this research synthesized the V/TS-1 by adding the vanadium compound in A1, A2, C1, C2 solution and both of A1 and A2 solution.

4.2 Catalyst characterization

The synthesized V/TS-1 catalysts were characterized by necessary techniques to clarify the catalyst structure, the morphology and the surface composition. The characterization results of synthesized catalysts are shown as follow:

4.2.1 X-ray fluorescence spectroscopy (XRF)

The chemical compositions of the synthesized catalysts were analyzed by x-ray fluorescence spectroscopy. Firstly, the catalysts that synthesized from three different methods of vanadium salt addition (i.e. adding VCl_3 in A1 solution, A2 solution, both of A1 and A2) are initially characterized to investigate the amount of vanadium in the structure using XRF technique. The results showed that the catalyst synthesized by adding VCl_3 in A1 solution has the highest quantity of vanadium incorporated into the TS-1 structure follow by the others those are synthesized by adding VCl_3 in both of A1 and A2 solution and only in A2 solution, respectively.

This means that the majority of vanadium in catalyst structure is derived from the gel solution. Therefore, the effects of synthesis methodology (the vanadium salt addition method) of other types of vanadium salt (VCl_3, $VO(acac)_2$ and V_2O_5) are investigated by adding the vanadium salt in each solution used to prepare the gel solution (i.e. A1, B1 and C1 solution) and adding in both of A1 and A2 solution.

The chemical compositions and the atomic ratio of Si/Ti and Si/V of the V/TS-1 samples are presented in Table 4.2. The detail calculations of these values are illustrated in Appendix C.

Table 4.2 The chemical compositions of the cations and the atomic ratio of Si/Ti and Si/V of V/TS-1 samples. (% by mole)

Samples	%Si	%Ti	%V	Si/Ti	Si/V
VCl_3_A1	99.545	0.192	0.279	517.9989	355.8621
VCl_3_A2	99.709	0.251	0.013	464.0446	7498.0779
VCl_3_A1A2	99.461	0.232	0.262	428.5394	379.1923
VCl_3_C1	99.507	0.200	0.293	497.9750	339.6178
$VO(acac)_2$_A1	99.219	0.261	0.445	379.8346	223.1783
$VO(acac)_2$_A1A2	99.567	0.225	0.167	443.1816	596.7476
V_2O_5_A1	99.678	0.241	0.014	414.2178	7307.0764
V_2O_5_A1A2	99.683	0.228	0.015	437.7095	6781.4817
V_2O_5_C1	99.743	0.256	0.00009	389.1680	1054361

The results showed that the V/TS-1 catalysts which synthesized from the same vanadium source but different in vanadium salt addition method and vice versa have different quantity of vanadium. This is likely due to the fact that each vanadium salt provides different forms of cation and anion complex when dissolve in water. The dissolution of VCl_3 in water gives the hexahydrate ion, $[V(H_2O)_6]^{3+}$ which has green colour. $VO(acac)_2$ is a coordination complex between the vanadyl cation, VO^{2+}, and

two acetylacetonate anions, acac$^-$. When dissolve in water, the salt dissipated in to VO^{2+} cation (more accurately [VO(H$_2$O)$_5$]$^{2+}$) and two acetylacetonate anions, acac$^-$. The dissolution of V$_2$O$_5$ investigated in this study gives the orange-colored solution in the pH range between 9 and 11. This implies that the prepared solution contains mainly the ions HVO$_4$$^{2-}$ and V$_2$O$_7$$^{4-}$. It should be emphasized here that, in an aqueous solution, V^{5+} tends to stay in the negative ions.

As mentioned above, considering the prepared solutions obtained from VCl$_3$ and VO(acac)$_2$, the vanadium species in both solutions exist in the part of cation complex, whereas those obtained from V$_2$O$_5$ are presented in the part of anion complex. Table 4.2 shows that the amounts of vanadium incorporated into TS-1 structure of the catalysts synthesized from VCl$_3$ and VO(acac)$_2$ are higher than those synthesized from V$_2$O$_5$. According to this result, it can be concluded that it is easier for the vanadium species exist in the part of cation complex which probably have smaller molecule than the one presented in the part of anion complex to incorporated into the TS-1 structure. The highest and the lowest quantity of vanadium could be incorporated into the TS-1 structure are about 0.445 and 0.00009 mole% of total cations found in VO(acac)$_2$_A1 and V$_2$O$_5$_C1, respectively.

4.2.2 X-ray diffraction (XRD)

The XRD diffraction patterns of each sample are shown in Figure 4.1. The crystal of each type of zeolite has different characteristic peaks. Hence, the XRD pattern can be used to identify the structure of the zeolite. The characteristic peaks describing the MFI structure appear at 2θ as 8, 8.8, 14.8, 23.1, 24 and 29.5 respectively (Zhao et al., 2000). From Figure 4.1, the XRD patterns of all synthesized V/TS-1 samples have the same characteristic peak as the MFI structure of the TS-1 (six main characteristic peaks marked with dark circle) this means all of them have MFI structure. Therefore, it can be concluded that the vanadium salt addition method and the type of vanadium salt do not significantly affect the MFI structure.
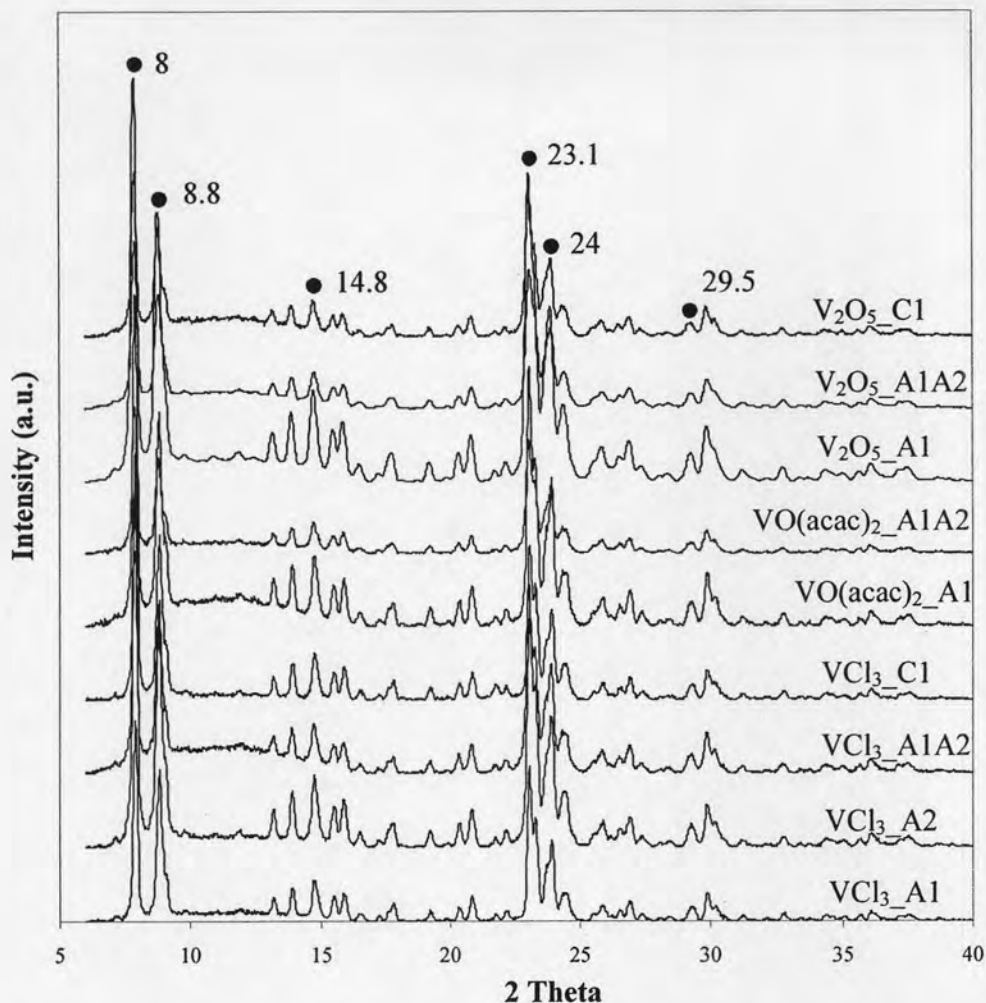
Figure 4.1 The XRD diffraction patterns of the V/TS-1 samples

4.2.3 Fourier-transform infrared spectroscopy (FT-IR)

To investigate SiO_2 framework, fourier transform infrared spectroscopy, FT-IR, was used in this study. The defection of SiO_2 framework can be revealed at 900-1000 cm^{-1} region. Smooth spectrum, no peak appear, at that region indicate that our catalyst framework is composed of SiO_2 only, if not, some defections occur in our framework. (Perego et al., 1986). From the previous research, it has been reported that the absorption band around 960-975 cm^{-1} indicates that Ti^{4+} exists in silicate framework (Huybrechts et al., 1991). Figure 4.2 represents the IR spectra of the synthesized V/TS-1, it is clearly seen that some peaks appear around 960-975 cm^{-1}.

Therefore, it can be concluded that all synthesized V/TS-1 catalysts have Ti^{4+} in silicate framework the same as the TS-1 catalyst.
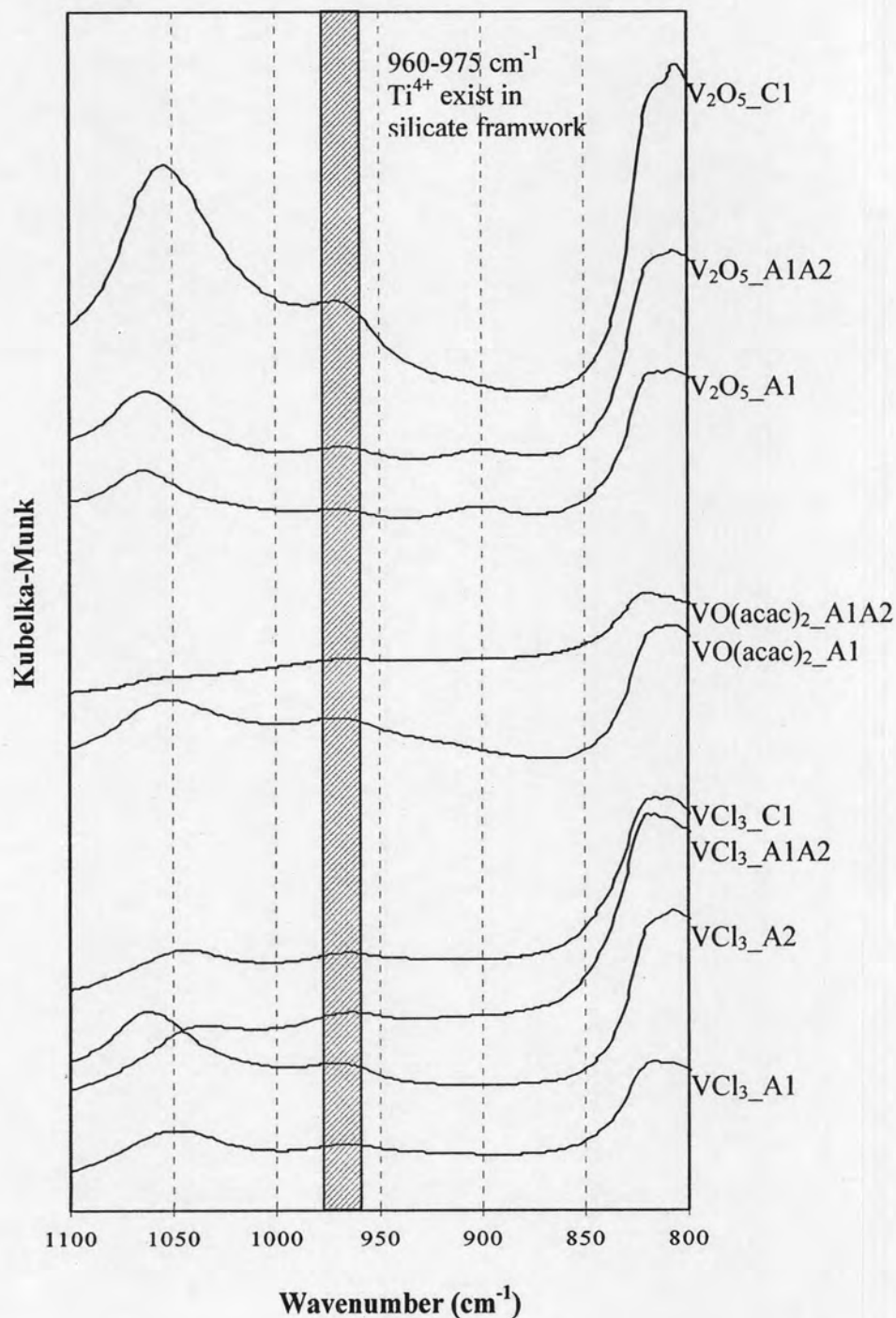
Figure 4.2 IR spectra of the synthesized V/TS-1 catalysts

4.2.4 Brunaur-Emmett-Teller (BET) surface area, pore volume and pore sized analysis

The surface area, pore volume and pore size of V/TS-1 samples are presented in Table 4.3. The sample with higher amount of vanadium has lower surface area. It is assumed that the vanadium added into TS-1 may exists in the framework and extraframework, (such as pore and surface of V/TS-1). Therefore, the surface area of all V/TS-1 samples decrease.

Table 4.3 Surface area, pore volume and pore size of V/TS-1 samples

Sample	A_{BET} (m^2/g)	Pore volume (cm^2/g)	Pore size (Å)
VCl$_3$_A1	292.333	0.161	22.075
VCl$_3$_A2	319.933	0.225	28.124
VCl$_3$_A1A2	299.711	0.194	25.846
VCl$_3$_C1	272.116	0.163	23.955
VO(acac)$_2$_A1	276.463	0.168	24.325
VO(acac)$_2$_A1A2	309.786	0.204	26.388
V$_2$O$_5$_A1	297.959	0.216	29.030
V$_2$O$_5$_A1A2	307.458	0.217	28.266
V$_2$O$_5$_C1	323.249	0.222	27.485

4.2.5 Scanning electron microscopy (SEM)

SEM micrographs of the synthesized V/TS-1 samples are shown in Figure 4.3. A similar type of morphology is observed in all samples. It reveals that the shapes of all catalysts are roughly crystallized orthorhombic shape and the crystal sizes are in the range of 3-5 micron. It is observed that the amount of vanadium incorporated into TS-1 lattice does not greatly alter the shape of the crystals.
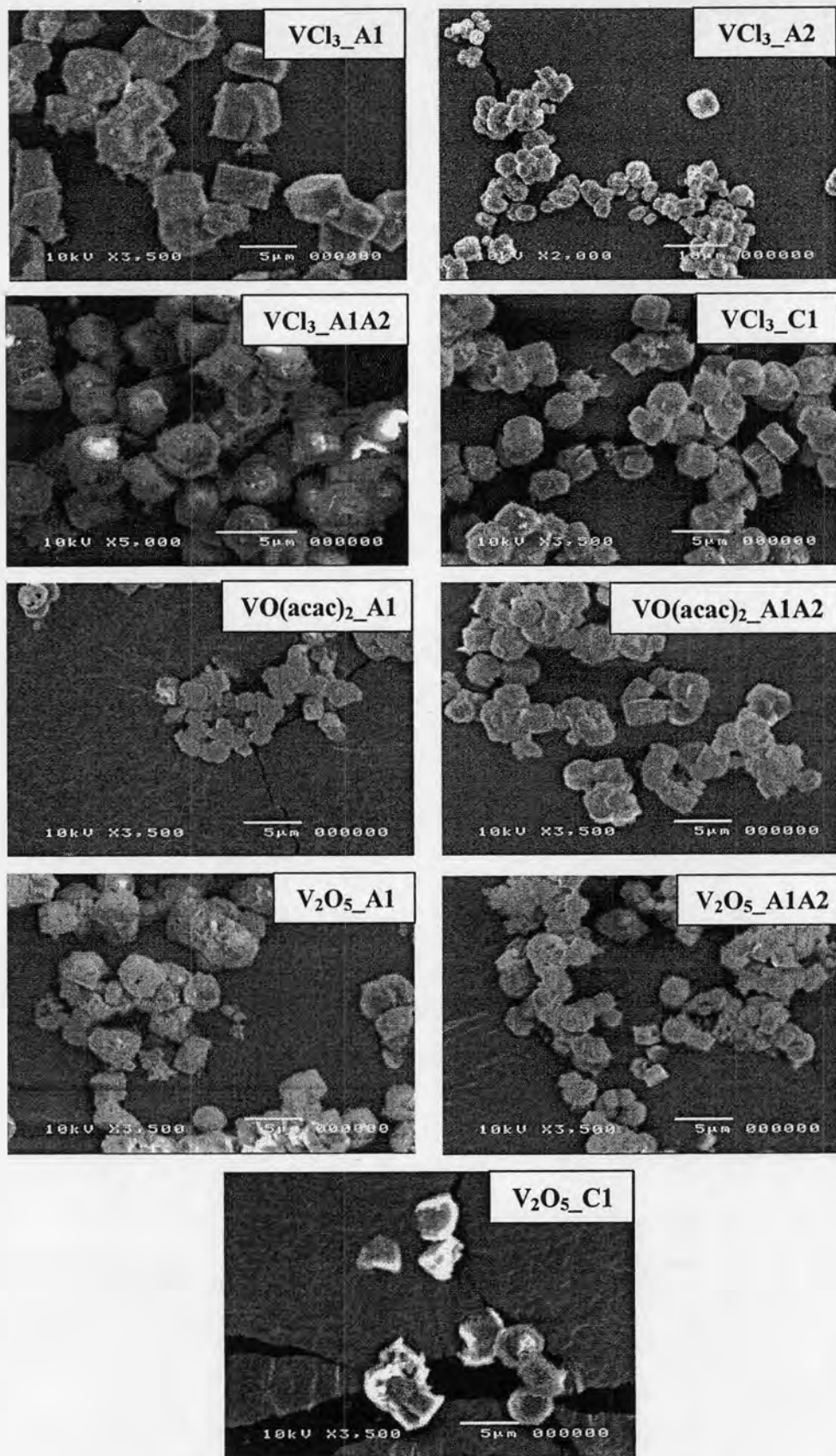
Figure 4.3 SEM micrograph of V/TS-1 samples

4.2.6 Electron spin resonance (ESR)

The ESR technique was applied to investigate the vanadium species presented within zeolite framework. It has been reported that the vanadium species existing in the framework is likely to be V^{+5} species since V^{+5} has no signal when detected by the ESR technique (Whittington and Anderson, 1991). Figure 4.4 shows the ESR spectra of all synthesized V/TS-1 samples at 25°C. This observation presented all samples did not display the ESR signal; this indicated that all of them consist of the V^{+5} species in the TS-1 lattice. Since all V/TS-1 samples were synthesized from different vanadium sources which contain vanadium in different oxidation states but the ESR results of all samples are similar. Therefore, the explanation is required. In the preparation procedure, all V/TS-1 samples were calcined in air to eliminate impurity. In this step the V^{3+} and V^{4+} species may be oxidized completely to more stable V^{+5} species (Julbe et al., 2000).
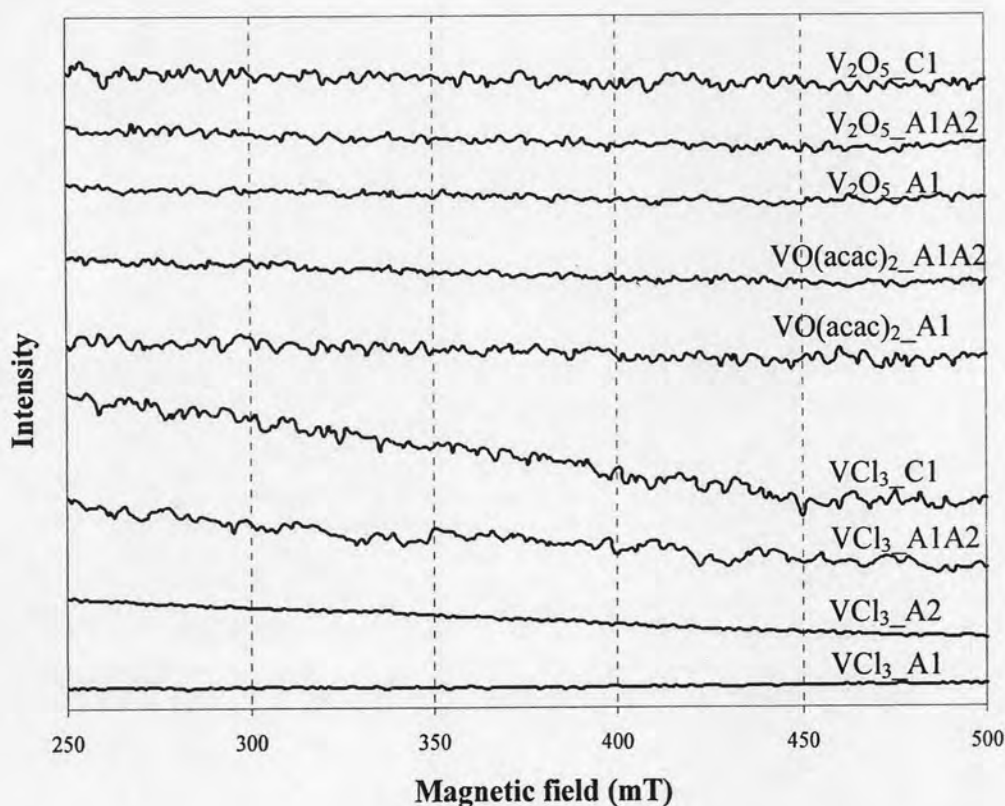
Figure 4.4 X-band ($\upsilon = 9.43$ GHz) powder spectra at 25°C representative of the V/TS-1 samples

4.2.7 NH₃-Temperature programmed desorption (NH₃-TPD)

The TPD profiles of the V/TS-1 catalysts are based on the desorption temperature maxima which could be divided into two regions corresponding to a weaker (135-145°C) and a stronger acid strengths (222- 242°C) as representative in Figure 4.5.
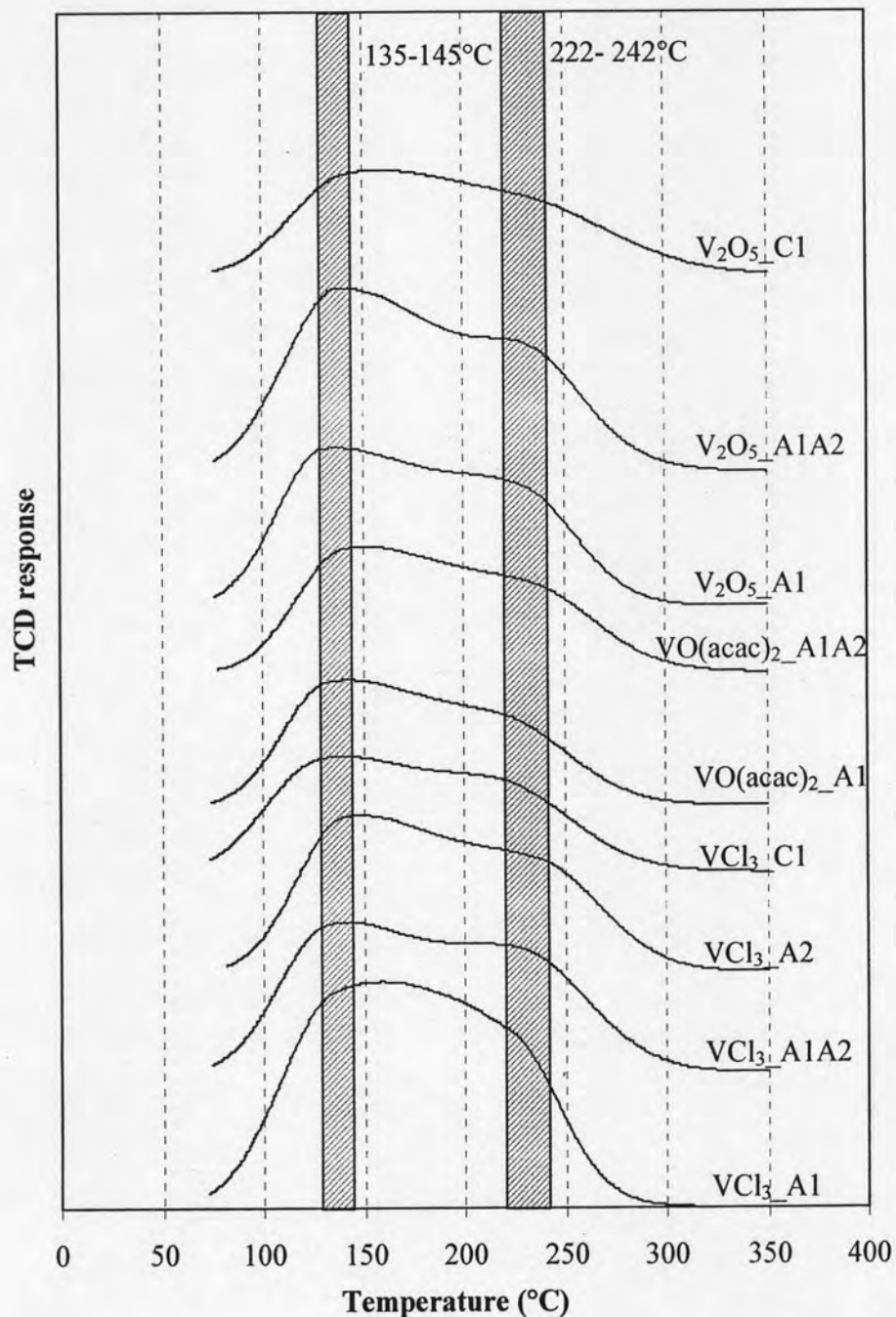

Figure 4.5 NH₃-TPD of V/TS-1 samples

To find the quantities of acid sites and acid strength on the catalyst surface, the results which are calculated from raw data of NH_3-TPD with some helps of peak fitting program presented in Appendix D are presented in Table 4.4

Table 4.4 Desorption temperature and acid site quantities of the synthesized V/TS-1 samples

Sample	Weak acid site		Strong acid site		Total acid site (μmol/g)
	Temp (°C)	Site (μmol/g)	Temp (°C)	Site (μmol/g)	
VCl_3_A1	141	179	229	82	261
VCl_3_A2	135	96	230	73	169
VCl_3_A1A2	145	121	242	50	171
VCl_3_C1	135	85	229	27	112
$VO(acac)_2$_A1	137	122	229	31	153
$VO(acac)_2$_A1A2	137	48	222	48	96
V_2O_5_A1	135	110	232	47	157
V_2O_5_A1A2	143	144	237	33	177
V_2O_5_C1	145	65	236	42	107

4.3 The catalytic reaction

The catalytic performance of the synthesized catalysts was evaluated by using the gas phase oxidation of 2-propanol as a test reaction. The catalytic results (i.e. percent conversion of 2-propanol, mole of 2-propanol used and mole of each product formed) of all synthesized catalysts, the effect of vanadium on the combustion and on the oxidation of 2-propanol are discussed as follow:

4.3.1 Catalytic activity in gas phase oxidation of 2-propanol

The conversion of V/TS-1 samples in the gas phase oxidation of 2-propanol are divided into three sets of vanadium source (i.e. VCl_3, $VO(acac)_2$ and V_2O_5). The variation in 2-propanol conversion of the catalysts synthesized with the same vanadium source and different vanadium salt addition methods are illustrated in Figures 4.6-4.8.
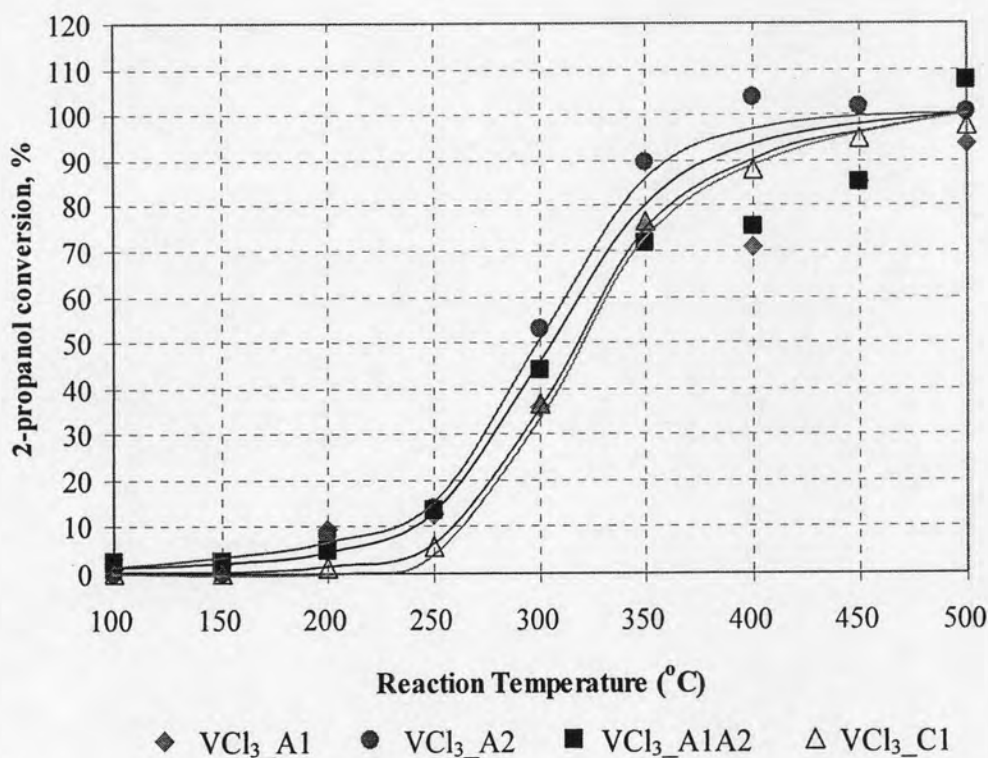
Figure 4.6 Variation of conversion with reaction temperature for VCl_3_A1, VCl_3_A2, VCl_3_A1A2 and VCl_3_C1
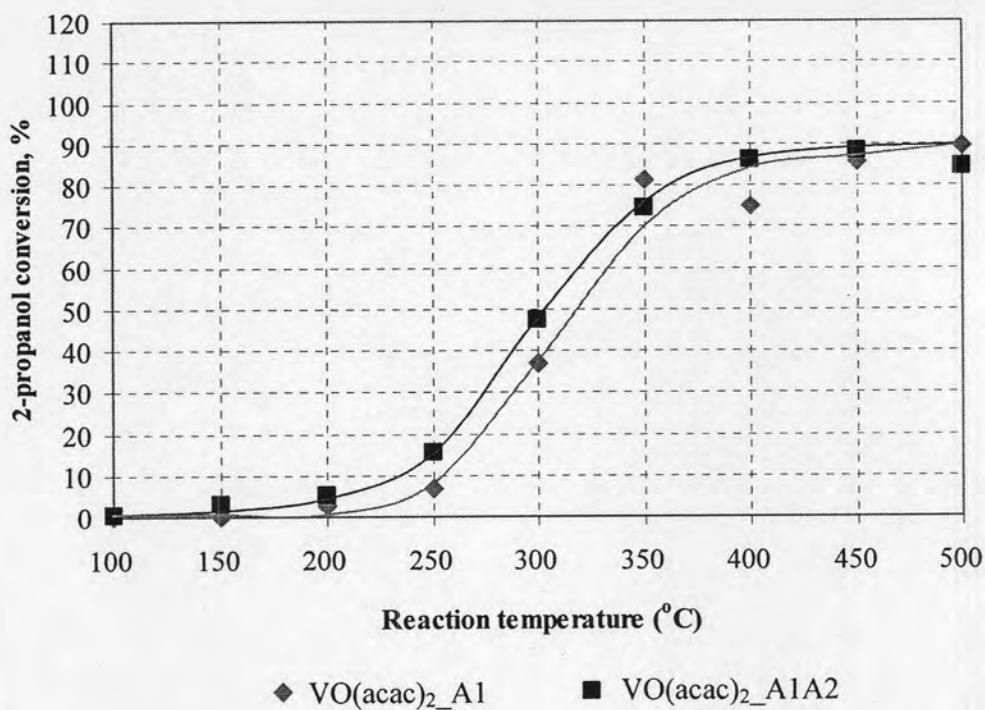
Figure 4.7 Variation of conversion with reaction temperature for VO(acac)$_2$_A1 and VO(acac)$_2$_A1A2
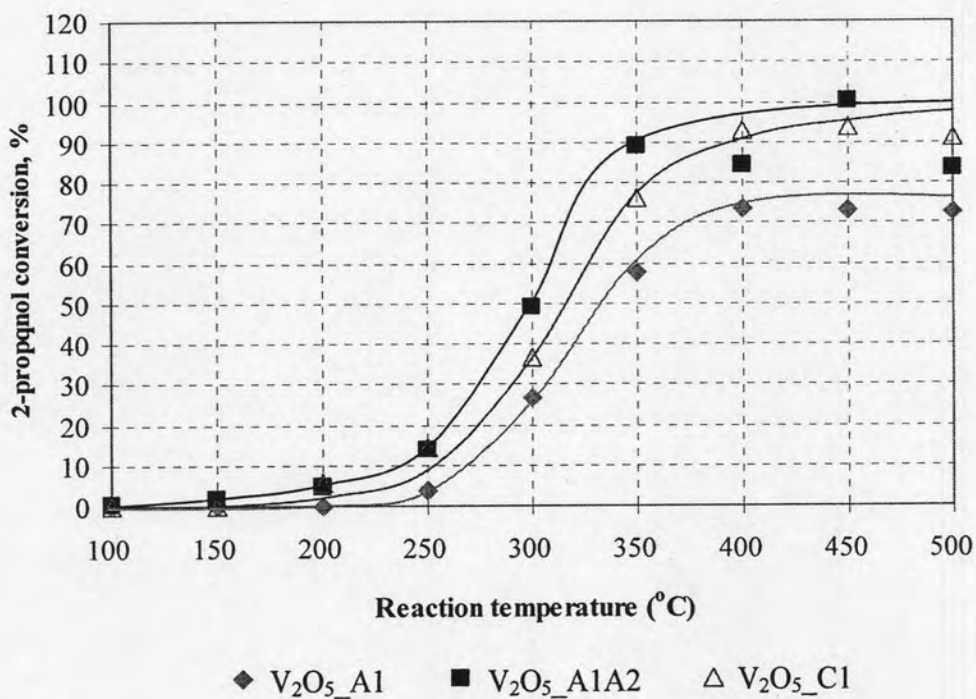

Figure 4.8 Variation of conversion with reaction temperature for V$_2$O$_5$_A1, V$_2$O$_5$_A1A2 and V$_2$O$_5$_C1

Figure 4.6 reports the variation in 2-propanol conversion of four catalysts synthesized with the same vanadium source (VCl_3) and different vanadium salt addition method as a function of reaction temperature. The general trend is that whatever the vanadium salt addition method is, the conversion of all samples are almost identical at high temperature, 500°C (nearly 100%). For VO(acac)$_2$_A1 and VO(acac)$_2$_A1A2, the increasing rate of the conversion of the latter is faster than the former. Both of them give approximately 90% conversion at 500°C as represented in Figure 4.7. The conversions of catalysts synthesized by using V_2O_5 as a source of vanadium are shown in Figure 4.8. It was found that the conversion of V_2O_5_A1 is significantly lower compared to V_2O_5_A1A2 and V_2O_5_C1. Moreover, the increasing rate of the conversion of V_2O_5_A1A2 at low and intermediate temperature is faster than V_2O_5_C1. However, both of them give the same order conversion at high temperature, 500°C.

Figures 4.6-4.8 imply that the catalysts synthesized by adding the vanadium salt in A2 solution which is used to prepare the decant solution give the highest 2-propanol conversion although these catalysts have the lowest quantity of vanadium incorporated into the TS-1 structure. This is probably due to the vanadium species dissolved in the decant solution may precipitate mainly on the surface of the catalysts and give the shell catalyst with an extremely thin shell. The vanadium specie on the surface is more active than the one present in the framework because it is easier for the reactant to penetrate into the vanadium active site. In case of the catalysts synthesized by adding the vanadium salt in the solutions (i.e. A1 and C1 solution) used to prepare the gel solution give higher quantity of incorporated vanadium, lower in 2-propanol conversion. This is probably from the reason that most of the vanadium species is embedded in the framework rather than exist on the surface of the catalyst. The predicted vanadium distributions in the structure of catalysts synthesized by adding the vanadium salt in the gel solution and those adding in the decant solution are illustrated in Figures 4.9a and 4.9b.
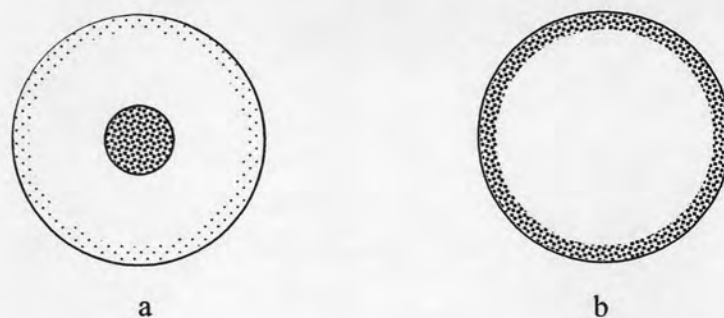
Figure 4.9 The predicted vanadium distributions in the structure of catalysts

a) synthesized by adding the vanadium salt in the gel solution

b) synthesized by adding the vanadium salt in the decant solution

4.3.2 Catalytic selectivity in gas phase oxidation of 2-propanol

Since 2-propanol can be reacted to provide many products (e.g. propylene, acetone, isopropyl ether and carbondioxide). Therefore the reaction pathways of this reactant must be investigated. The catalytic results of all synthesized catalysts shown in term of mole of reactant used and mole of each product formed are displayed in Figures 4.10-4.18.
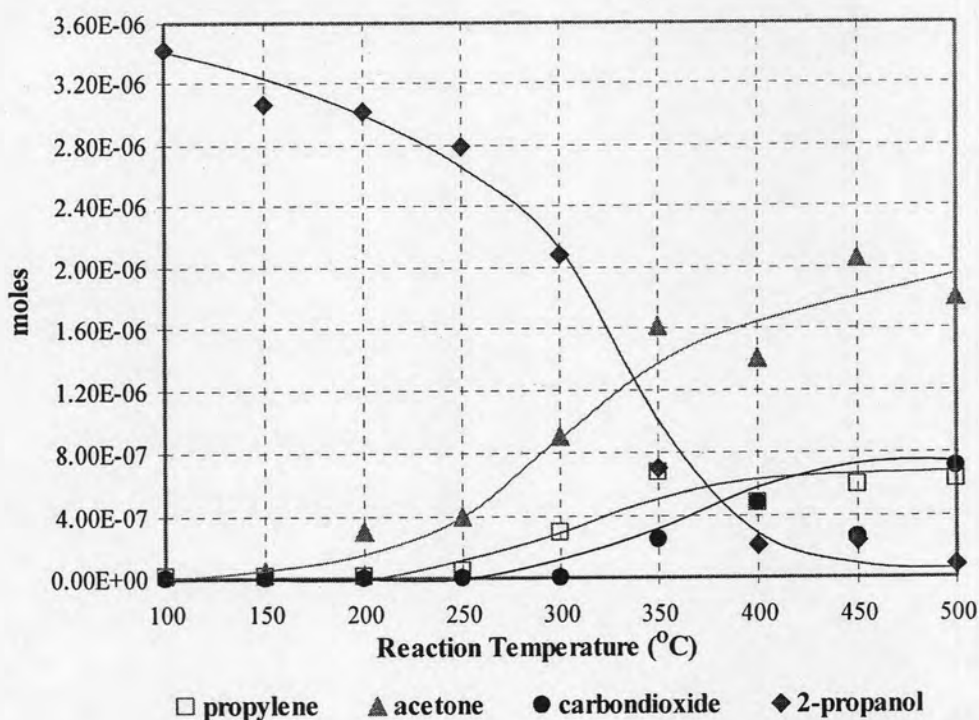
Figure 4.10 The catalytic selectivity of VCl_3_A1
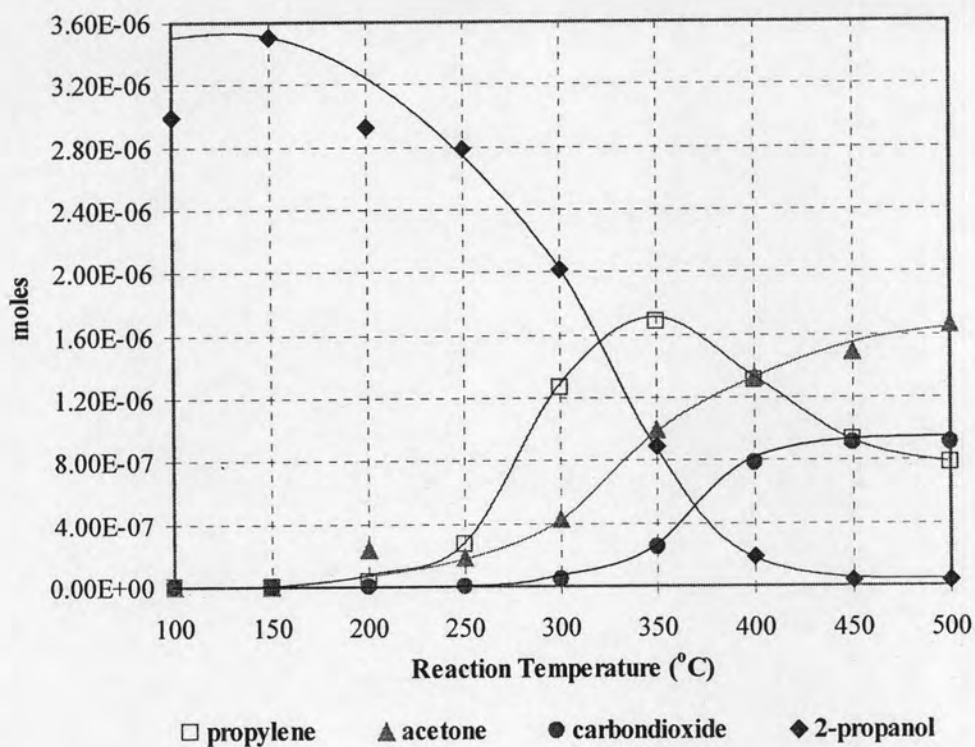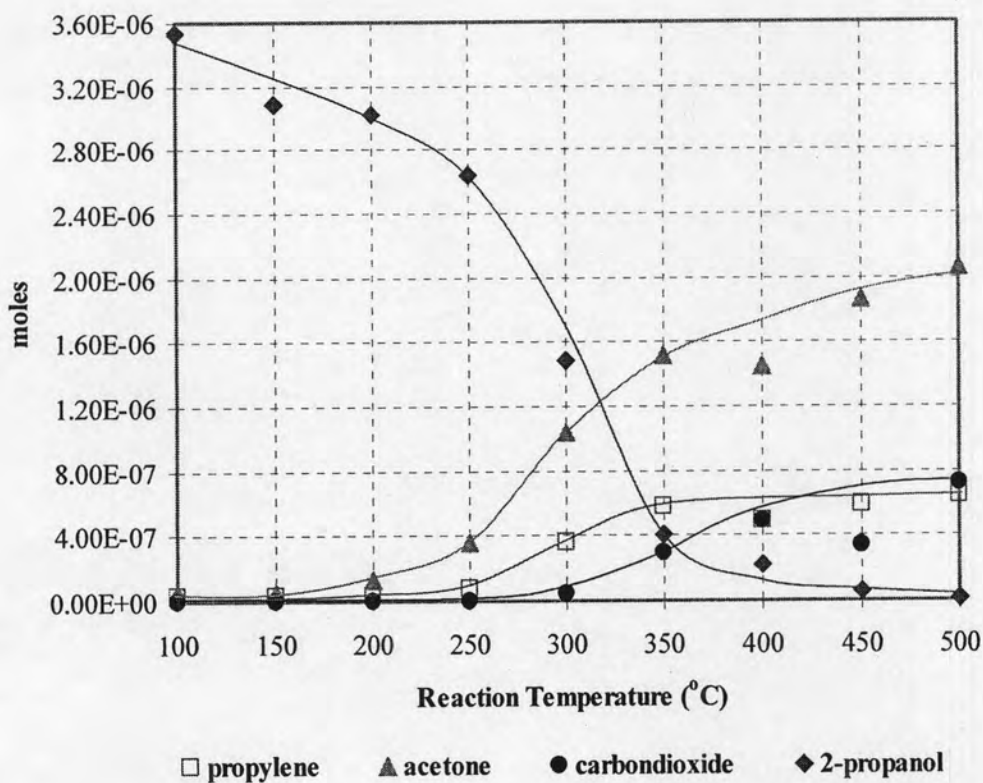
Figure 4.11 The catalytic selectivity of VCl$_3$_A2

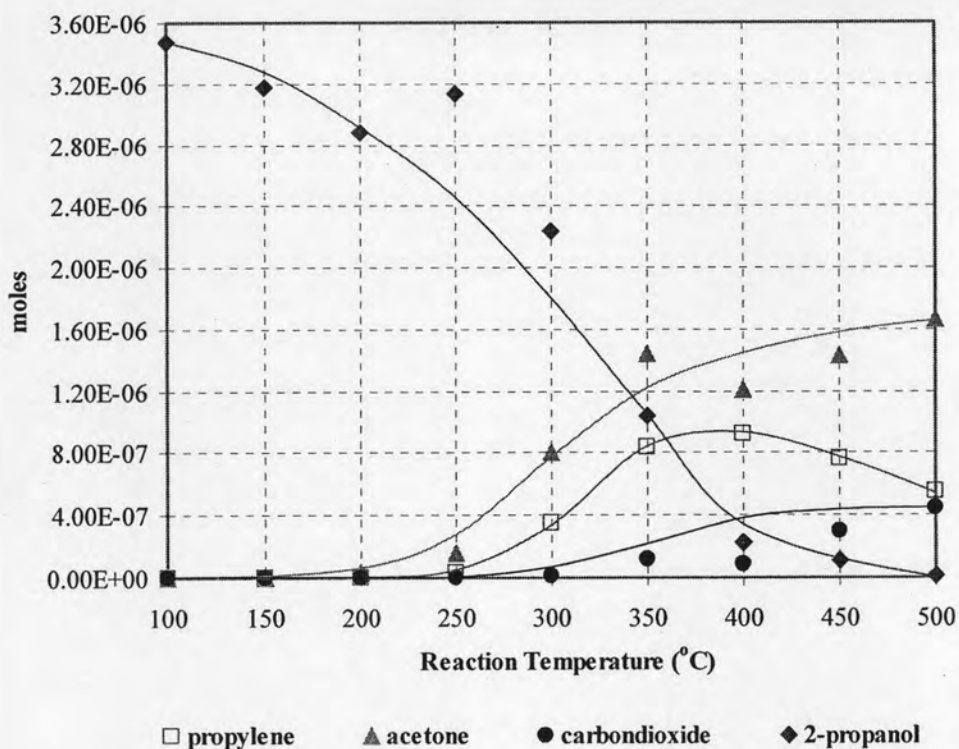**Figure 4.12** The catalytic selectivity of VCl$_3$_A1A2
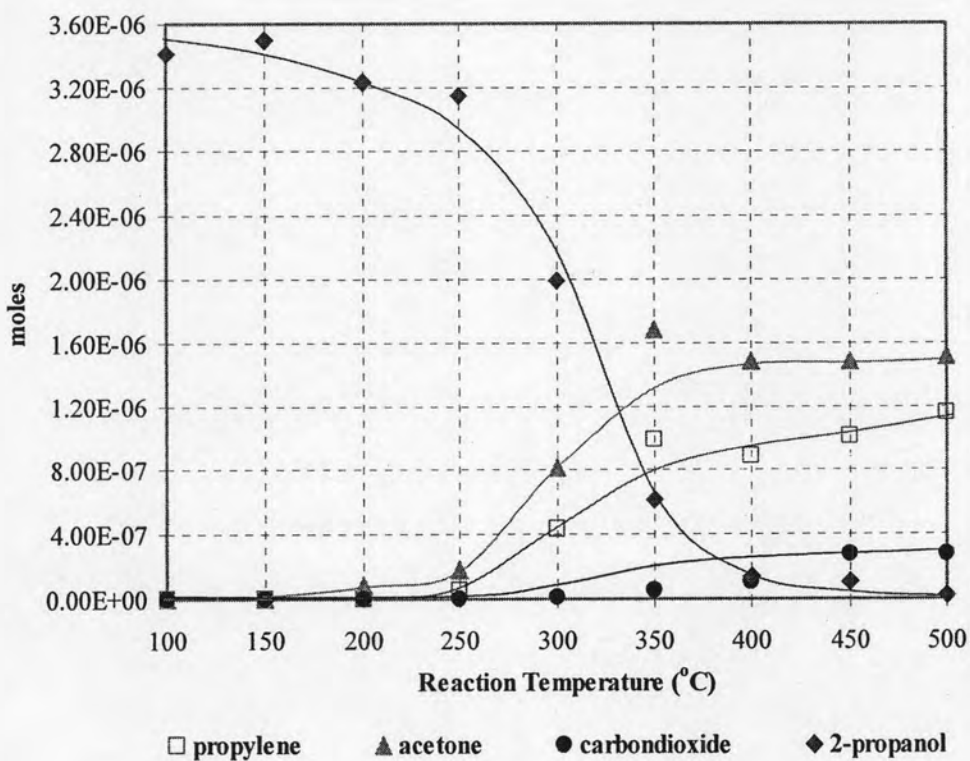
Figure 4.13 The catalytic selectivity of VCl_3_C1
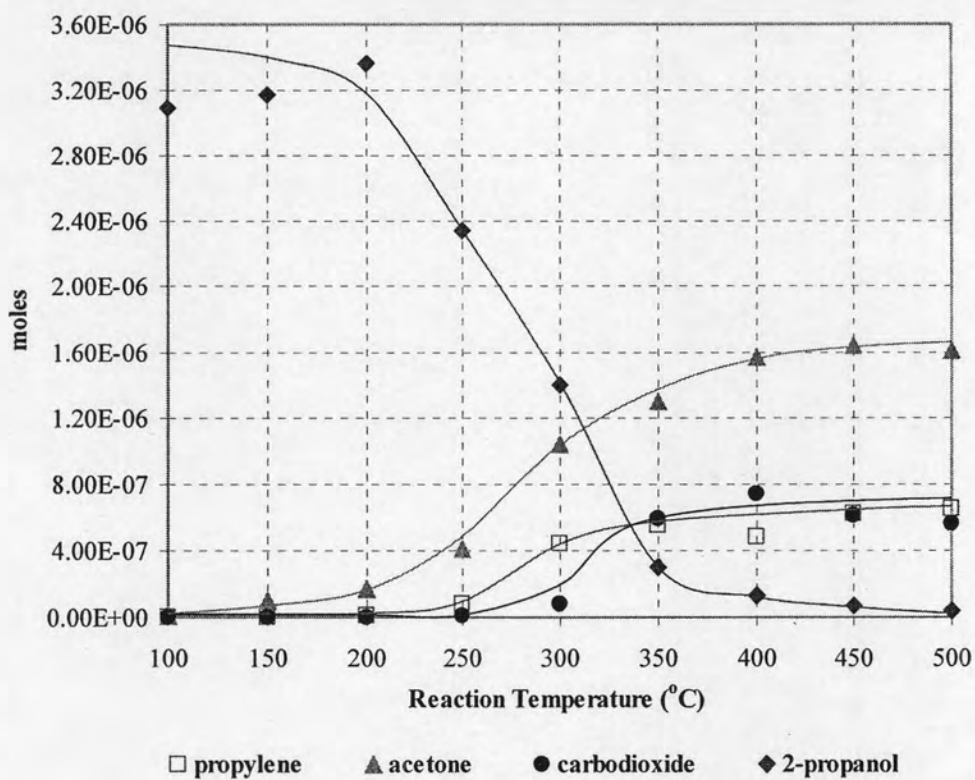

Figure 4.14 The catalytic selectivity of $VO(acac)_2\_A1$

Figure 4.15 The catalytic selectivity of VO(acac)$_2$_A1A2
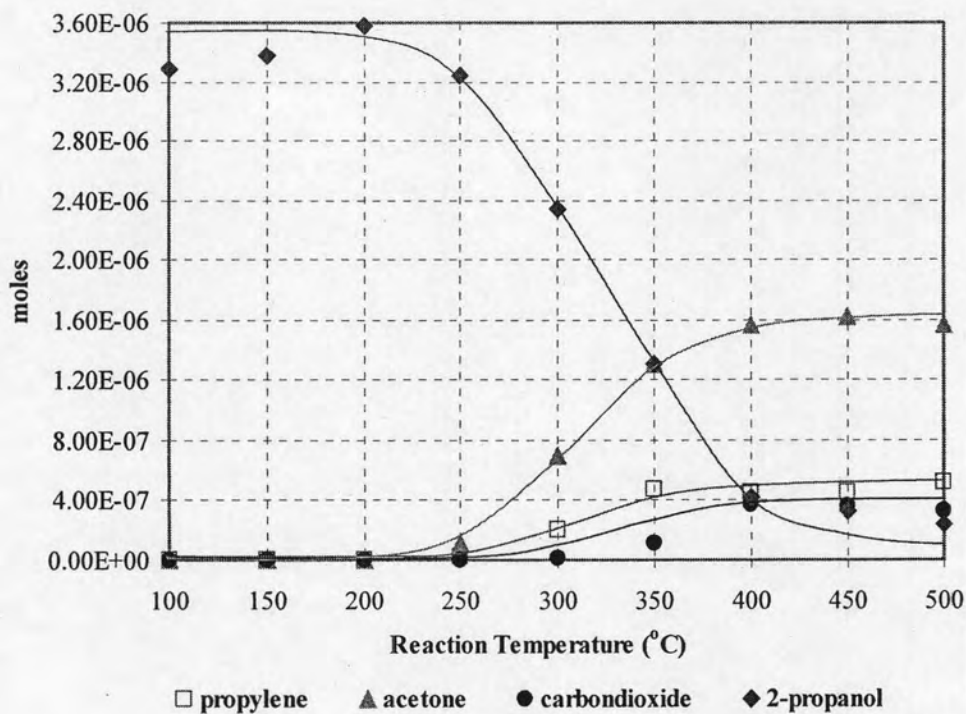
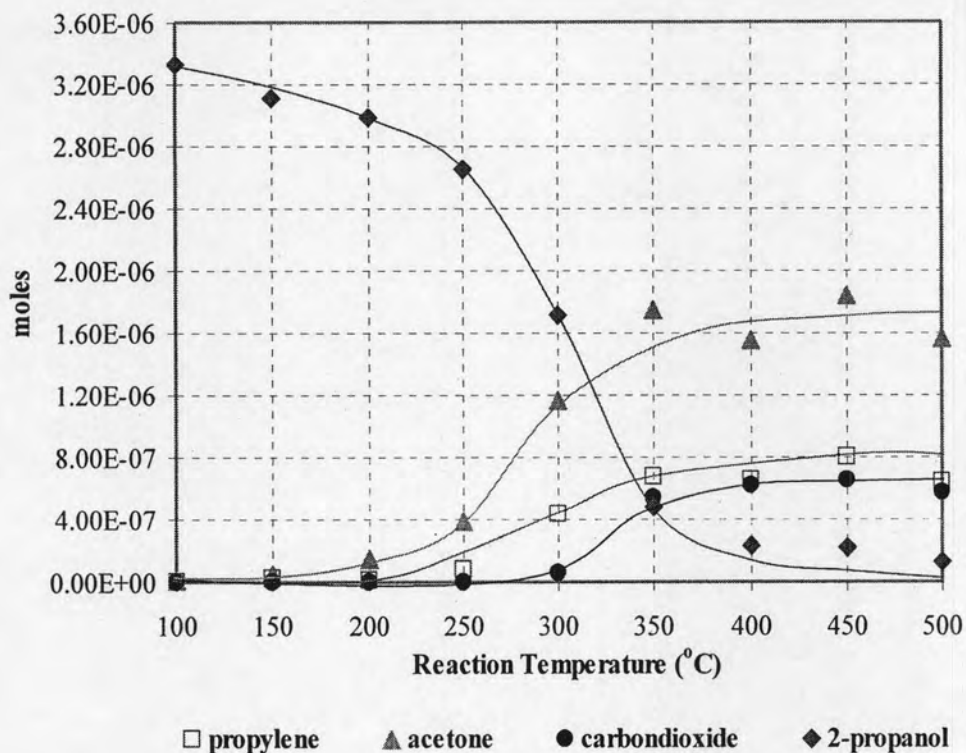**Figure 4.16** The catalytic selectivity of V$_2$O$_5$_A1

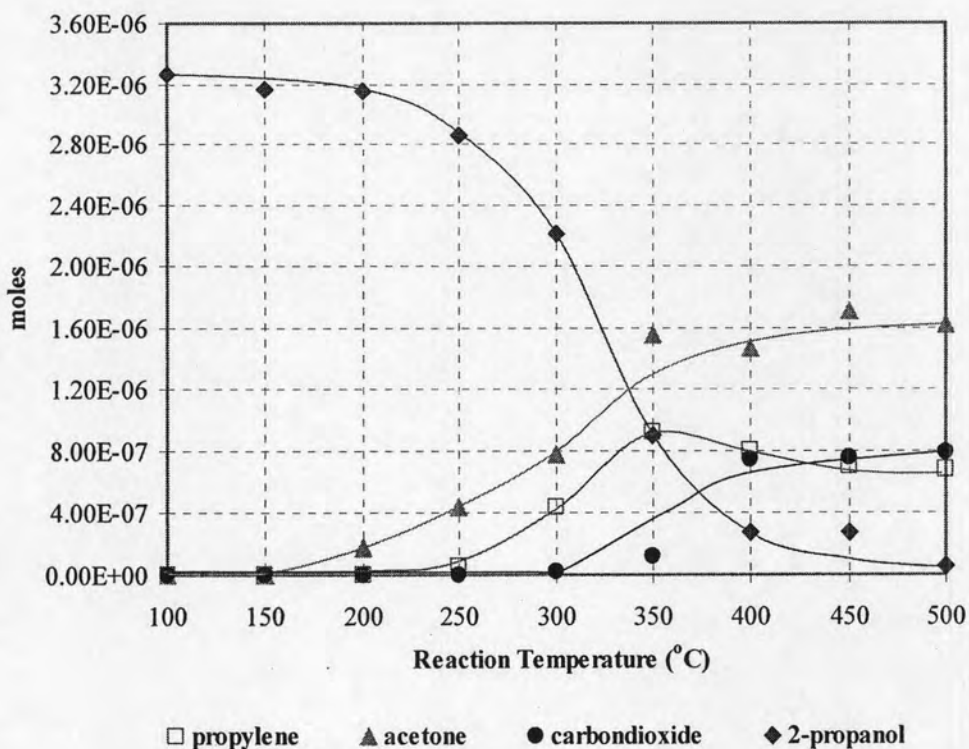**Figure 4.17** The catalytic selectivity of $V_2O_5\_A1A2$

Figure 4.18 The catalytic selectivity of $V_2O_5\_C1$

For all samples, acetone was initially produced at the reaction temperature 100°C. Propylene was also produced at 100°C while carbondioxide became significant at the reaction temperature above 300°C. The quantities of isopropyl ether formed were very small; hence, it was neglected for this consideration. The maximum amount of carbondioxide was obtained at the reaction temperature range, $400-500^{\circ}$C. 2-propanol can be dehydrated to produce propylene and oxidized to produce acetone. Carbondioxide maybe produced via the combustion of 2-propanol directly or produced via the combustion of acetone and propylene. The reaction pathway over all samples is likely to be the same as found in the previous work that used TS-1 as a catalyst (Chairat, 2004). The catalytic results show that the reaction pathways of all synthesized catalysts are similar. Therefore, it can be concluded that the vanadium salt addition and the type of vanadium salt do not significantly affect the reaction pathway. The reaction pathway of 2-propanol is illustrated in Figure 4.19.
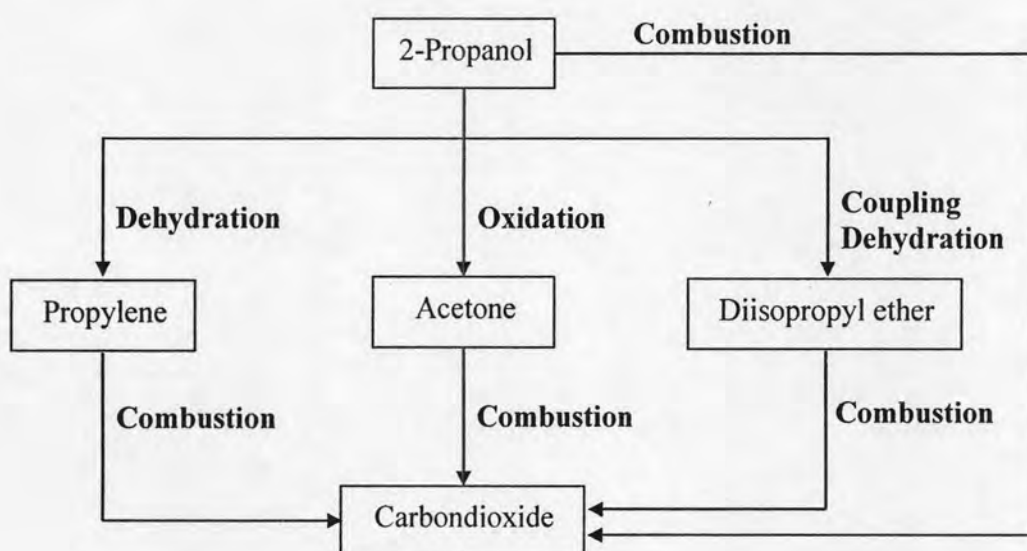

Figure 4.19 The reaction pathway of 2-propanol

Since the different vanadium sources which contain vanadium in different oxidation states provide different vanadium cation or anion complexes when dissolved in water during the synthesis procedure. Therefore, the active vanadium species with different oxidation states bonded on the surface of the synthesized catalysts before calcination in the air stream may form different surface structures.

After calcination in the air stream at 550 °C for 7 hours, the synthesized catalysts which contain the same V^{5+} species bonded in different forms on the surface were obtained. These different forms of vanadium active species may have different catalytic behaviors for the gas phase oxidation of 2-propanol. Hence, the catalytic selectivity over these synthesized catalysts is divided into three sections by the type of vanadium salts used (i.e. VCl_3, $VO(acac)_2$ and V_2O_5). The catalytic selectivities including the expanded discussions are discussed as follow:

4.3.2.1 Vanadium (III) chloride (VCl_3)

Figure 4.11 shows the catalytic selectivity of VCl_3_A2 catalyst which contains the smallest amount of incorporated vanadium species. It is found that this catalyst gives the highest quantity of propylene and carbondioxide formed compared with the ones found in VCl_3_A1, VCl_3_A1A2 and VCl_3_C1 (Figures 4.10, 4.12 and 4.13) which contain higher amount of incorporated vanadium. These results imply that the incorporated vanadium species play an important role in the decrease of the dehydration of 2-propanol to form propylene as a product. Moreover, it is found that the incorporated vanadium species open the route for the selective oxidation of 2-propanol as seen from the selectivity to acetone over the synthesized catalysts which increases with the amount of incorporated vanadium. Since the 2-propanol oxidation uses oxygen as a reactant and can take place in the whole range of temperature from 100 to 500°C, therefore the higher oxidation to produce acetone must consume more amount of oxygen resulting in the small amount of oxygen remaining in the reaction system. This is the explanation why the formation of carbondioxide from the 2-propanol combustion which is found at high temperature over 300°C is lower when the 2-propanol oxidation is predominant.

4.3.2.2 Vanadyl acetylacetonate ($VO(acac)_2$)

The catalytic selectivity of $VO(acac)_2$_A1 which contains 0.261 mole% Ti and 0.445 mole% V was compared with the one of $VO(acac)_2$_A1A2 that contains 0.225 mole% Ti and 0.167 mole% V. The amount of vanadium in the former is much higher than in the latter. Figures 4.14 and 4.15 present the acetone selectivity of both catalysts are almost identical and the carbondioxide selectivity over

VO(acac)$_2$_A1 is higher than over VO(acac)$_2$_A1A2, this implies that the vanadium active species derived from VO(acac)$_2$ bonded on the catalyst surface do not be active in the 2-propanol oxidation but it can inhibit the 2-propanol combustion. The increase of propylene over VO(acac)$_2$_A1 is probably due to the effect of titanium active species existing in the catalyst surface.

4.3.2.3 Vanadium (V) oxide (V$_2$O$_5$)

Since the catalysts synthesized from V$_2$O$_5$ contain small amount of incorporated vanadium species, therefore the consideration about the effect of vanadium species in the 2-propanol oxidation is neglected. In addition, the amounts of titanium in these catalysts are nearly similar. Figures 4.16 - 4.18 show that the product selectivities over all catalysts are almost identical. It can be concluded that the product selectivities over these catalysts only depend on the titanium active species existing on the catalyst surface.

According to the results discussed above, different vanadium sources contain vanadium in different oxidation states provide different vanadium cation or anion complexes which have different abilities to incorporate into the TS-1 structure when dissolved in water during the synthesis procedure. Moreover, the active vanadium species from different vanadium complex ions bonded on the catalyst surface probably form the dissimilar structures which subsequently result in different catalytic behaviors. Therefore, it can be concluded that the type of vanadium salt significantly affects the amount of vanadium specie incorporated into the TS-1 structure as well as the catalytic activity in the gas phase oxidation of 2-propanol.